Liquid Crystals
Publication details, including instructions for authors and subscription information:
http://www.informaworld.com/smpp/title~content=t713926090

Dynamics of the field-induced twist deformation in weakly anchored nematic layers

Grzegorz Derfel; Barbara Gajewska

Online publication date: 29 June 2010

To cite this Article Derfel, Grzegorz and Gajewska, Barbara(1997) 'Dynamics of the field-induced twist deformation in weakly anchored nematic layers', Liquid Crystals, 22: 3, 297 — 300
To link to this Article: DOI: 10.1080/026782997209351
URL: http://dx.doi.org/10.1080/026782997209351

LIQUID CRYSTALS, 1997, VOL. 22, NO. 3, 297–300

Dynamics of the field-induced twist deformation in weakly anchored nematic layers

by GRZEGORZ DERFEL*, BARBARA GAJEWSKA
Institute of Physics, Technical University of Łódź, ul. Wólczańska 223, 93-005 Łódź, Poland

(*Received 27 June 1996; in final form 17 October 1996; accepted 30 October 1996*)

The dynamics of the field-induced one-dimensional twist deformation in weakly anchored nematic layers was investigated by means of numerical simulation. The rise time constants and the decay time constants, characteristic for the onset and for the decay of the deformation, respectively, were determined. The time of delay, which had passed before the decay started, was revealed in the case of finite anchoring. For weaker anchoring, the time of delay and the decay time constant were longer. Surprisingly, the onset of the deformation was slower when the anchoring was weaker, provided that the ratio of the actual field strength to the threshold field strength was fixed.

1. Introduction

The dynamics of field-induced deformations in nematic layers are governed by several factors:

(i) The properties of the material, expressed by its elastic constants, viscosity coefficients and dielectric (diamagnetic) anisotropy.
(ii) The parameters of the layer, namely its thickness, the energy of the surface anchoring and the surface orientation.
(iii) The external field strength and direction.

Some of these factors influence both the onset and the decay of the deformation.

The transient phenomena due to the field-induced deformations have usually been examined experimentally under strong anchoring conditions (e.g. [1]). In the theoretical analysis, infinite anchoring energy was assumed and the possibility of deformations in the regions adjacent to the surfaces was ignored [2]. In the present paper, the simplest case of the pure twist deformation is considered. Its dynamics are modelled numerically. The characteristic times, which describe the transient effects are distinguished as follows:

— the rise time constant characterizing the exponential development of the deformation,
— the decay time constant describing the exponential relaxation to the undeformed state,
— the delay time, which passes after switching off the field and before the decay starts.

One would expect that a weak anchoring energy would manifest itself in a faster onset of deformation and by a slower relaxation to the uniform state. However, our calculations reveal the opposite character for the rise process: the rise time constant under stronger anchoring conditions is smaller than in the case of weaker surface interactions, provided that in both cases the time constants are compared for the same ratio of the field strength to the threshold value.

2. Method

To study the effect of weak (finite) anchoring energy on the dynamics of the field-induced transition, the simplest type of deformation was chosen. A planar nematic layer of thickness d, parallel to the (xy) plane was considered. The magnetic field $\mathbf{H}=(H\,0\,0)$ was directed perpendicular to the initial director orientation $\mathbf{n}(0\,1\,0)$ and parallel to the layer plane. In such a geometry, the resulting deformation consists of pure twist, the transient phenomena are free from any backflow effect and the problem is not complicated by the spatial dependence of the internal field. The actual director distribution in the deformed layer is described by the time-dependent angle $\theta(z,t)$, measured between the $\mathbf{n}$ vector and the y axis. The nematic liquid crystal was characterized by the elastic constant k_{22}, the twist viscosity γ and the small positive diamagnetic anisotropy $\Delta\chi$. The boundary plates were placed at $z=\pm d/2$. The initial uniform director field was due to the aligning effect of the surfaces described by the easy axis $\mathbf{e}(0\,1\,0)$ and by the Rapini–Papoular anchoring free energy

$$F_{\text{anchoring}}=-(W/2)(\mathbf{ne})^2 \tag{1}$$

Analysis of the static deformations induced by external

*Author for correspondence.

fields in weakly anchored homogeneous layers has revealed the existence of two threshold fields, [3,4]. The layer remains undeformed until the lower threshold H_1 is reached. Above the higher threshold, H_2, the director is uniformly aligned along the field. These results apply to the present geometry.

The director dynamics are investigated in two cases: when the deformation arises after the sudden onset of the field of strength exceeding the lower threshold, and when the deformation decays after abruptly switching off the field, which was previously in equilibrium with the deformed stationary structure. The former process is described by the torques equation

$$\frac{\partial^2\theta}{\partial z^2}=\Delta\chi H^2\sin\theta\cos\theta=\gamma\frac{\partial\theta}{\partial t}, \qquad (2)$$

and the latter process by the equation

$$\frac{\partial^2\theta}{\partial z^2}=\gamma\frac{\partial\theta}{\partial t}. \qquad (3)$$

In both cases, the following boundary conditions should be satisfied.

$$\left.\frac{\partial\theta}{\partial z}\right|_{\pm d/2}\pm\frac{Wd}{k_{22}}\sin 2\theta(\pm d/2)=\gamma\frac{\partial\theta}{\partial t} \qquad (4)$$

In the present paper the solution of the problem is obtained numerically. For this purpose, the actual $\theta(z,t)$ function is approximated by a set of $N\times M$ discrete values θ_{ij} ($i=1\ldots N$, $j=1\ldots M$). They are due to the N equidistant planes which divide the layer into $N-1$ sublayers, and to M values of time, measured after switching on (or off) the field. By means of these discrete angles, the expressions equivalent to equations (2) to (4) are derived. The solution is obtained using some iteration procedure. It starts from some initial set of θ_{i1}. At each step, the new value θ_{ij+1} is calculated by use of θ_{i-1j}, θ_{i+1j} and θ_{ij} values. This procedure is repeated until the whole set of θ_{ij} remains practically unchanged during subsequent iterations. In our calculations, $N=65$ and $M=150$, which gives satisfactory approximation of the actual $\theta(z,t)$ dependence.

3. Results

The results presented in the following are obtained for the nematic material with $k_{22}=8\times10^{-12}$ N and $\gamma=0{\cdot}1\,\mathrm{N\,s\,m^{-2}}$. The layer thickness $d=15\times10^{-6}$ m is chosen. The anchoring energy is characterized by the dimensionless parameter $g=Wd/2k_{22}$. Several values of g are considered in the simulation. The typical form of both the development and the decay of the deformation is shown in figure 1 by means of the $\theta(z,t)$ functions. Figure 2 shows the mid-plane angle $\theta(z=0,t)\equiv\theta_m(t)$ and the boundary angle $\theta(z=\pm d/2,t)\equiv\theta_b(t)$ plotted as functions of time. Figure 3 presents logarithms of the angles. The relatively high magnetic field is chosen for these plots in order to reveal the delay time, corresponding to switching off the field higher than H_2. The exponential increase and decrease of the angles are evident if their magnitudes are sufficiently far from the saturation values, i.e. at an early stage of the onset and at the final stage of the decay, respectively. The slopes of the inclined linear segments of the curves serve to determine the time

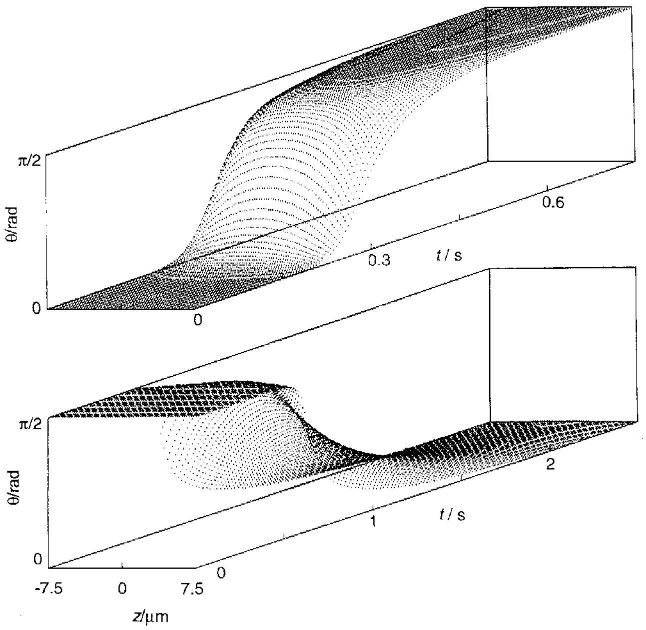

Figure 1. The $\theta(z,t)$ function for the rise of deformation (above) and for the decay of deformation (below); $g=5$, $h^*=16{\cdot}5$, $H>H_2$.

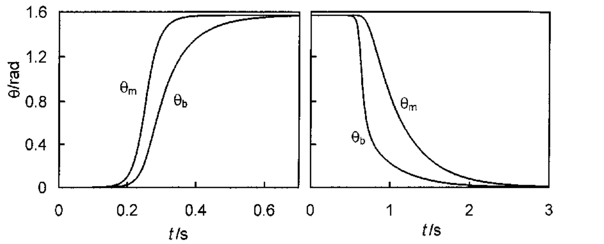

Figure 2. The mid-plane angle θ_m and the boundary angle θ_b as functions of time after the onset of the field (left) and after switching of the field (right); $g=5$, $h^*=16{\cdot}5$, $H>H_2$.

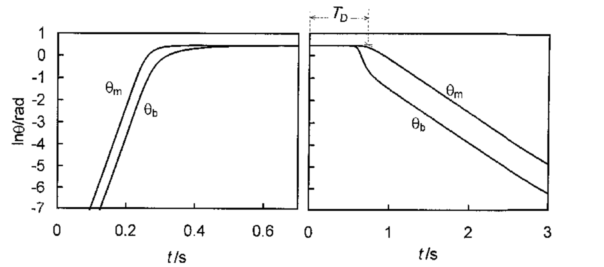

Figure 3. The logarithm of the angles θ_m and θ_b after the onset of the field (left) and after switching of the field (right) plotted as functions of time; $g=5$, $h^*=16{\cdot}5$, $H>H_2$.

constants τ_R for the rise of the deformation and τ_D for its decay. In figure 3, the time of delay T_D is defined. In the following, the mid-plane angle is used to represent the behaviour of the layer.

The rise time constant depends on the surface anchoring energy and on the magnetic field strength which is illustrated in figures 4 and 5. Figure 4 shows the proportionality of $1/\tau_R$ to the parameter $h^*=(H^2-H_1^2)/H_1^2$ plotted for several anchoring strengths. The slopes of the plots are lower for smaller anchoring energy parameters. This means that for given h^* the rise time constant is bigger when the anchoring is weaker. This

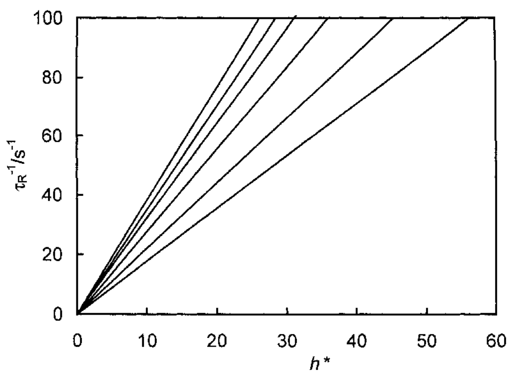

Figure 4. The inverse rise time constant $1/\tau_R$ as a function of the field excess parameter h^* plotted for $g=2$, 3, 5, 10, 20 and 100 000 (in order from the lowest slope to the highest slope).

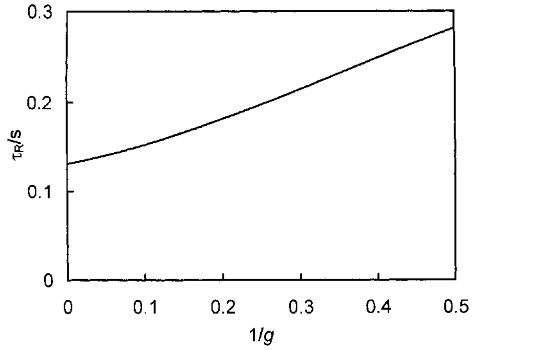

Figure 5. The rise time constant τ_R as a function of the inverse anchoring energy parameter $1/g$ for $h^*=2$.

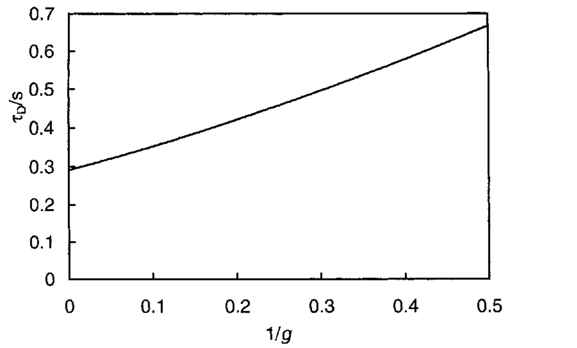

Figure 6. The decay time constant τ_D as a function of the inverse anchoring energy parameter $1/g$.

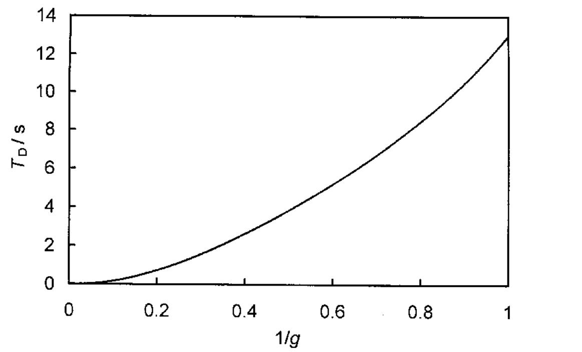

Figure 7. The delay time T_D as a function of the inverse anchoring energy parameter $1/g$.

tendency is illustrated in figure 5, which shows, that for given h^* the stronger anchoring assures the faster onset of deformation.

The decay time constant τ_D grows if the anchoring becomes weaker; this is shown in figure 6. In addition, the delay time T_D is revealed for finite g. Figure 7 shows its increase with $1/g$.

4. Discussion

In this paper, the dynamics of the uniform deformations induced by a magnetic field were analysed. The twist distortions were considered as the simplest example. Two-dimensional distortions, which occur in the form of periodic patterns (see, e.g. [5] and the references cited therein) are beyond the scope of our work.

In the case of infinitely strong anchoring, the time dependences of the mid-plane angle during its rise and decay are expressed by series of exponential components with different time constants [2]. The slowest component is described by the time constants

$$\tau_R^{\mathrm{theor}} = \frac{\gamma d^2}{\pi^2 k_{22} h^*} \quad (5)$$

for the development of the deformation and by

$$\tau_D^{\mathrm{theor}} = \frac{\gamma d^2}{\pi^2 k_{22}} \quad (6)$$

for the decay.

In the case of finite anchoring energy, the rise time constant depends both on the anchoring parameter g and on the magnetic field strength. It is reasonable to consider the $\tau_R(g)$ dependence for a constant field excess above the lower threshold in order to assure comparable conditions for layers with different anchoring energies. Here, the ratio H/H_1 included in the parameter h^* was adopted as a natural measure of this quantity, which is justified by its presence in formula (5). With this choice, an apparently surprising result is obtained: for fixed h^*, the weaker anchoring gives the slower onset of deformation. (The more intuitive $\tau_R(g)$ dependence with faster onset dynamics, under weaker anchoring conditions, can be obtained, if the magnetic field strength H is chosen instead of the ratio H/H_1.)

For very strong anchoring, the final stage of the onset of deformation is very well described by an exponential time dependence and the time constants for $\theta_m(t)$ and $\theta_b(t)$ are the same. For weak anchoring, however, the exponential dependence is limited to a rather short period. Therefore the dynamics of the deformation are described here by analysis of the $\theta_m(t)$ function, when it is sufficiently far from saturation value.

The proportionality constant for the linear relation between $1/\tau_R$ and h^*, presented in figure 4 for practically stiff anchoring ($g = 10\,000$) differs from the value obtained from equation (5). The computed time constant is about 8 per cent smaller than τ_R^{theor}, probably due to the contribution of faster components. The similar difference for the decay time constant amounts to about 2 per cent.

References

[1] Van Dijk, J. W., Beens, W. W., and De Jeu, W. H., 1983, *J. chem. Phys.*, **79,** 3888.
[2] Brochard, F., Pierański, P., and Guyon, E., 1972, *Phys. Rev. Lett.*, **28,** 1681.
[3] Nehring, J., Kmetz, A. R., and Scheffer, T. J., 1976, *J. appl. Phys.*, **47,** 850.
[4] Derfel, G., 1991, *Liq. Cryst.*, **10,** 29.
[5] Winkler, B. L., Richter, H., Rehberg, I., Zimmermann, W., Kramer, L., and Buka, A., 1991, *Phys. Rev. A*, **43,** 1940.